Frustrated Resonating Valence Bond States in Two Dimensions: Classification and Short-Range Correlations

Fan Yang[1] and Hong Yao[2,3]

[1]School of Physics, Beijing Institute of Technology, Beijing, 100081, China
[2]Institute for Advanced Study, Tsinghua University, Beijing, 100084, China
[3]Department of Physics, Stanford University, Stanford, California 94305, USA

(Received 10 May 2012; published 5 October 2012)

Resonating valence bond (RVB) states are of crucial importance in our intuitive understanding of quantum spin liquids in 2D. We systematically classify short-range bosonic RVB states into symmetric or nematic spin liquids by examining their flux patterns. We further map short-range bosonic RVB states into projected BCS wave functions, on which we perform large-scale Monte Carlo simulations without the minus sign problem. Our results clearly show that both spin and dimer correlations decay exponentially in all the short-range *frustrated* (nonbipartite or Z_2) bosonic RVB states we studied, indicating that they are gapped Z_2 quantum spin liquids. Generically, we conjecture that *all* short-range frustrated bosonic RVB states in 2D have only short-range correlations.

DOI: 10.1103/PhysRevLett.109.147209 PACS numbers: 75.10.Kt

Introduction.—Quantum spin liquids are exotic insulators which cannot be adiabatically connected into a band insulator and which can support fractionalized excitations [1]. Introduced by Anderson nearly four decades ago [2], the resonating valence bond (RVB) state on the triangular lattice is the first example of quantum spin liquids in more than one dimension. Since then, there has been keen interest in searching for such exotic states of matter in real materials as well as in microscopic models, especially after exciting connections between quantum spin liquids and the mechanism of high temperature superconductivity were suggested [3–5].

Recently, there has been a surge of numerical simulations on simple models reporting convincing evidence of the existence of fully gapped spin liquids [6–11], all of which are believed to be in the same class of short-range bosonic RVB states. Nonetheless, the nature of short-range bosonic RVB states on various frustrated lattices has not been explicitly revealed [12,13], mainly because of the so-called minus sign problem in Monte Carlo (MC) simulations of those bosonic short-range RVB states with frustration. Because of their conceptual importance in pictorially understanding quantum spin liquids and their direct relevance in recent numerical simulations, it is highly desired to unambiguously demonstrate the nature of these short-range bosonic RVB states.

In this Letter, we systematically classify short-range bosonic RVB states by examining their flux patterns [14]. For instance, for the kagome lattice we establish that there are only four symmetric RVB states when considering only nearest-neighbor (NN) valence bonds, as is shown in Fig. 1. Then, we show that these bosonic short-range RVB states can be exactly mapped into projected BCS wave functions [15–17] on which we perform large-scale MC simulations without the minus sign. For frustrated short-range RVB states, our simulations on corresponding projected BCS states convincingly show that both their spin and dimer correlations decay exponentially, indicating that they are fully gapped Z_2 spin liquids [18,19].

Bosonic RVB states.—We consider the following bosonic RVB states with NN and possibly next-nearest-neighbor (NNN) valence bonds

$$|\psi_{\mathrm{RVB}}\rangle = \sum_c |c\rangle, \qquad |c\rangle = (-1)^{\delta_c} \prod_{(ij)\in c} f_{ij}|ij\rangle, \tag{1}$$

where c labels valence bond configurations and δ_c represents the number of bond crossings in c [the factor $(-1)^{\delta_c}$ is nontrivial only for RVB states with valence bonds beyond nearest-neighbor sites]. Here, $|ij\rangle \equiv (|\uparrow_i\downarrow_j\rangle - |\downarrow_i\uparrow_j\rangle)/\sqrt{2}$ is the spin-singlet wave function (or valence bond) on (ij) and we assume $|f_{ij}|$ to respect all the lattice symmetries. Note that Eq. (1) represents a "bosonic" RVB state in the sense that $|\uparrow_i\downarrow_j\rangle = |\downarrow_j\uparrow_i\rangle$. Since $|ij\rangle = -|ji\rangle$, it is sufficient to consider $f_{ij} = -f_{ji}$. The wave function in Eq. (1) possesses a gauge symmetry: $|\psi_{\mathrm{RVB}}\rangle$ is invariant, up to a phase, under the transformation $f_{ij} \to e^{i\alpha_i} f_{ij} e^{i\alpha_j}$. In the following, we focus on time reversal *invariant* RVB states for which all f_{ij} can be chosen as real; signs of f_{ij} can be represented by oriented arrows on graphs: an arrow pointing from i to j means that $f_{ij} > 0$, as is shown in Fig. 1. We further define flux $\phi_p = 0, \pi \pmod{2\pi}$ for plaquette p through

$$\prod_{(jk)\in p}^{cc} \mathrm{sgn}(f_{jk}) = \exp(i\phi_p), \tag{2}$$

where cc means that the counterclockwise order of (jk) is taken in the product above and sgn is the sign function. It is clear that ϕ_p is gauge invariant for even-length plaquettes p.

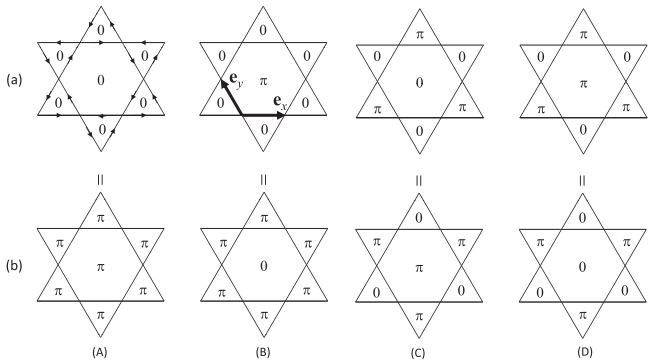

FIG. 1. (a) The flux patterns $\{\phi_p\}$ of the only four symmetric NN RVB states on the kagome lattice. Here, $\mathbf{e}_x$ and $\mathbf{e}_y$ represent the unit vectors. (b) The flux patterns $\{\phi_p^f\}$ in the corresponding projected BCS states.

However, the gauge transformation with $\exp(i\alpha_j) = i$ on every site j changes ϕ_p to $\phi_p + \pi$ for all odd-length plaquettes p. In other words, the two wave functions with flux patterns $\{\phi_p\}$ and $\{\phi_p + (-1)^{n_p}\pi\}$ (n_p is the length of plaquette p) actually represent the same state [20].

There are two questions to be answered concerning the wave function in Eq. (1). First, is it a symmetric spin liquid respecting all the symmetries of the lattice in question? Second, do various correlations decay in power law or exponentially? The first question can be answered by examining its flux pattern $\{\phi_p\}$. If the flux pattern $\{\phi_p\}$ is invariant up to the addition of $\{(-1)^{n_p}\pi\}$, under all lattice symmetry transformations such as translations, rotations, and reflections, the corresponding RVB state is then a symmetric spin-liquid state . We label RVB states whose longest valence bonds are between NN (NNN) sites as NN RVB (NNN RVB) states. On the kagome lattice, we identify four NN RVB states as symmetric spin liquids, as is shown in Fig. 1. On the triangular lattice, only two symmetric NN RVB states are found, as is shown in Fig. 2. On the square lattice, there are two symmetric NN RVB spin liquids and four symmetric NNN RVB states, as is shown in Fig. 3.

For these symmetric RVB spin liquids, it is not known *a priori* whether various correlations decay in power law or exponentially. Generically, numerical MC simulations are capable of revealing those features [21]. The correlations of a physical quantity O are given by

$$\langle O_i O_j\rangle = \frac{\langle\psi_{\mathrm{RVB}}|O_iO_j|\psi_{\mathrm{RVB}}\rangle}{\langle\psi_{\mathrm{RVB}}|\psi_{\mathrm{RVB}}\rangle} = \frac{\sum_{c,c'}\langle c|c'\rangle\left[\frac{\langle c|O_iO_j|c'\rangle}{\langle c|c'\rangle}\right]}{\sum_{c,c'}\langle c|c'\rangle}, \quad (3)$$

where $\langle c|c'\rangle$ ($|\langle c|c'\rangle|$) can be taken as statistical weight in MC simulations when they are positive (negative). For instance, for the square lattice NN RVB state with $\{\phi_p = 0\}$, $\langle c|c'\rangle \geq 0$ for any c and c', on which large-scale loop-algorithm MC simulations [22] were performed recently, reporting convincing evidence that this RVB state is critical with power-law decaying dimer corrections [23,24].

However, it is impossible to choose $\langle c|c'\rangle \geq 0$ for all c and c' for NN RVB states on nonbipartite lattices (e.g., the triangular lattice) or NNN RVB states on bipartite lattices (e.g., the square lattice). Such states are examples of frustrated RVB wave functions defined as ones whose valence bonds form nonbipartite graphs. It is clear that loop-algorithm MC simulations on frustrated RVB states suffer from the minus sign problem in the variational level. In the following, we shall show that the RVB states in Eq. (1) can be exactly mapped into Gutzwiller projected BCS states, which are friendly to MC simulations, without the minus sign problem.

Projected BCS states.—It was known that the variational Monte Carlo method has been quite successful in simulating Gutzwiller projected BCS wave functions. We consider the following projected BCS wave functions:

$$|\psi_{p-\mathrm{BCS}}\rangle = \mathcal{P}_G \exp\left[\sum_{(ij)} g_{ij}(c^\dagger_{i\uparrow}c^\dagger_{j\downarrow} - c^\dagger_{i\downarrow}c^\dagger_{j\uparrow})\right]|0\rangle, \quad (4)$$

where $c^\dagger_{i\sigma}$ are electron creation operators, $|0\rangle$ is the vacuum, $\mathcal{P}_G$ is the Gutzwiller projection onto singly occupied states, and $g_{ij} = g_{ji}$, which are assumed to be real. A similar gauge symmetry exists for the projected BCS wave functions: the wave function is invariant, up to a phase, under the transformations $g_{jk} \to \exp(i\alpha_j^f) g_{jk} \exp(i\alpha_k^f)$. For time reversal invariant states with real g_{jk},

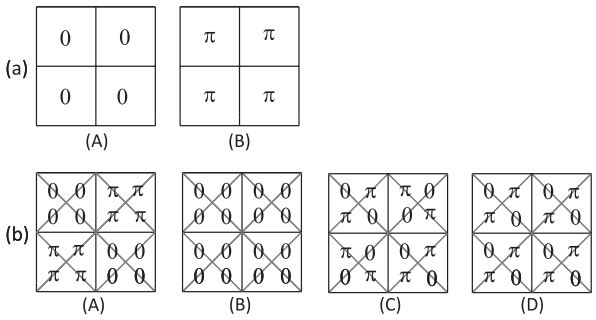

FIG. 3. The flux patterns $\{\phi_p\}$ of (a) the two symmetric NN RVB states and (b) the four symmetric NNN RVB states on the square lattice.

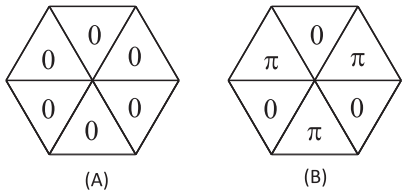

FIG. 2. The flux patterns $\{\phi_p\}$ of the two symmetric NN RVB states on the triangular lattice.

we define fermionic fluxes ϕ_p^f through $\prod_{(jk)\in p}\mathrm{sgn}(g_{jk}) = \exp(i\phi_p^f)$ with $\phi_p^f = 0, \pi \pmod{2\pi}$. Similarly, the flux patterns $\{\phi_p^f\}$ and $\{\phi_p^f + (-1)^{n_p}\pi\}$ are equivalent through the gauge transformation $\exp(i\alpha_j^f) = i$ on all sites j. As shown in detail in the Supplemental Material [25], we obtain $|\psi_{p-\mathrm{BCS}}\rangle = |\psi_{\mathrm{RVB}}\rangle$ when the following conditions are satisfied:

$$|g_{jk}| = |f_{jk}|, \qquad \phi_p = \phi_p^f + \pi, \tag{5}$$

where p labels all possible elementary plaquettes.

Ground-state correlations.—We have investigated a number of short-range frustrated RVB states by performing MC simulations on their corresponding projected BCS wave functions. In our numerical calculations, we mainly focus on spin as well as dimer correlations and study whether they fall off in power law or exponentially at large distances. The spin and dimer correlations are defined as follows:

$$S(\vec{l}) = \langle \mathbf{S}_{\vec{r}_i} \cdot \mathbf{S}_{\vec{r}_i+\vec{l}} \rangle,$$

$$D_\alpha(\vec{l}) = \langle (\mathbf{S}_{\vec{r}_i} \cdot \mathbf{S}_{\vec{r}_i+\mathbf{e}_\alpha})(\mathbf{S}_{\vec{r}_i+\vec{l}} \cdot \mathbf{S}_{\vec{r}_i+\vec{l}+\mathbf{e}_\alpha}) \rangle - \langle \mathbf{S}_{\vec{r}_i} \cdot \mathbf{S}_{\vec{r}_i+\mathbf{e}_\alpha} \rangle^2,$$

where $\mathbf{e}_\alpha$ labels lattice vectors.

We have studied all of the four symmetric NNN RVB states on the square lattice, the four symmetric NN RVB states on the kagome lattice, and the two symmetric NN RVB states on the triangular lattice. As discussed in detail later, for all these frustrated RVB states our MC simulations convincingly show that their spin and dimer correlations fall off exponentially with correlation length in the order of 1 lattice constant, indicating that they are all gapped Z_2 quantum spin liquids. (Note that different symmetric spin-liquid states on the same lattice may be distinguished by numerically computing local correlations.) We conjecture that our results are generic: all frustrated short-range RVB states in 2D are fully gapped.

The kagome lattice.—According to the flux pattern (either $\{\phi_p\}$ or $\{\phi_p^f\}$) on the kagome lattice, it is straightforward to show that there are four symmetric NN RVB spin liquids, as is shown in Fig. 1. We have computed the spin and dimer correlations for all of the four symmetric NN RVB spin liquids. In Fig. 4, we plot the spin and dimer correlations as a function of distance (l) in one of those NN RVB symmetric states, i.e., the counterclockwise-counterclockwise NN RVB state (A) shown in Fig. 1. The MC calculations are carried out on a lattice with $18 \times 18 \times 3$ sites and with periodic boundary conditions. It is remarkable that the correlations decay extremely fast. From Fig. 4, it is clear that both spin and dimer correlations decay exponentially at a distance. The spin correlation length ξ_s for this NN RVB state is about 0.6 lattice constants. The dimer correlation lengths $\xi_{d,x}$ and $\xi_{d,y}$ for $D_x(l\mathbf{e}_x)$ and $D_x(l\mathbf{e}_y)$ are nearly equal, which are about 1.2 lattice constants. The spin and dimer correlation lengths [ξ_s and $\xi_d \equiv (\xi_{d,x} + \xi_{d,y})/2$, respectively] for all of the four symmetric NN RVB spin liquids are listed in Table I. The correlation lengths are all in the order of 1 lattice constant, indicating that they are fully gapped Z_2 quantum spin liquids. This is consistent with the recent density matrix renormalization group evidence that the ground state of the kagome Heisenberg antiferromagnet is a fully gapped quantum spin liquid [8,9] with correlation lengths of about one lattice spacing [9].

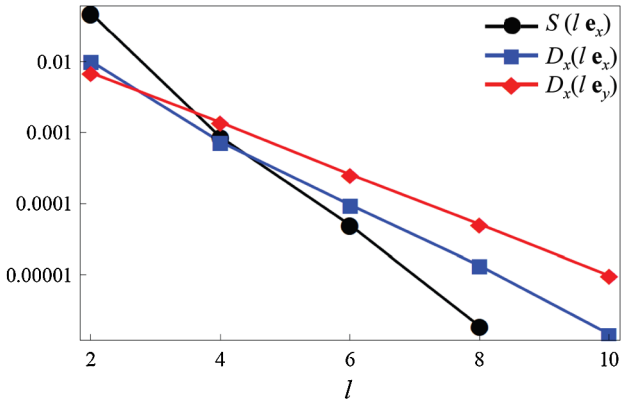

FIG. 4 (color online). The spin and dimer correlations as a function of distance in the NN RVB state (A) shown in Fig. 1.

To get a sense of which of the above states is the best variational wave function for the kagome antiferromagnet described by $H = J\sum_{\langle ij\rangle}\mathbf{S}_i \cdot \mathbf{S}_j$, we compute their variational energy per site, as is shown in Table I. Among the four symmetric NN RVB spin-liquid states, the counterclockwise-counterclockwise NN RVB state has the lowest energy for the kagome antiferromagnet, which is $-0.393J$ per site. This energy still differs from the density matrix renormalization group result, indicating that longer-range valence bonds are important in describing the kagome antiferromagnet.

The triangular lattice.—It turns out that there are only two symmetric NN RVB spin-liquid states on the triangular lattice, whose flux patterns $\{\phi_p\}$ are shown in Fig. 2. For both states, the spin and dimer correlations decay exponentially with distance, with $\xi_s = 0.7$ and $\xi_d = 1.0$ for state (A), shown in Fig. 2, and $\xi_s = 1.0$ and $\xi_d = 1.6$ for state (B), shown in Fig. 2. Both NN RVB states are then

TABLE I. The spin (ξ_s) and dimer (ξ_d) correlation lengths of the four symmetric states on the kagome lattice shown in Fig. 1. Here, E labels the variational energy per site of those symmetric states for the kagome NN antiferromagnetic Heisenberg model $H = J\sum_{\langle ij\rangle}\mathbf{S}_i \cdot \mathbf{S}_j$.

kagome NN RVB state	A	B	C	D
ξ_s	0.6	0.6	0.6	0.7
ξ_d	1.2	1.0	1.0	0.9
E/J	−0.393	−0.36	−0.357	−0.386

TABLE II. The correlation lengths and variational energies of the four symmetric NNN RVB states on the square lattice.

Square NNN RVB state	A	B	C	D
ξ_s	1.1	0.8	0.7	0.6
$\xi_{d,\mathrm{NN}}$	1.2	1.6	1.3	1.4
$\xi_{d,\mathrm{NNN}}$	0.6	0.6	0.6	0.5
E/J_1	−0.344	−0.219	−0.237	−0.239

gapped Z_2 spin liquids. The correlation lengths on the triangular lattice are somewhat longer than those on the kagome lattice, which is expected due to more geometric frustrations in the kagome lattice.

The square lattice.—It was shown recently that the unfrustrated NN RVB state on the square lattice is a critical state with power-law dimer correlations, even though its spin excitations are gapped [23,24,26]. To have a fully gapped spin-liquid phase on this lattice, it is necessary to include frustration in short-range RVB states. In this Letter, we consider to include NNN valence bonds, which is partly motivated by a recent study establishing that fully gapped spin-liquid ground states are realized in the generalized [27] quantum dimer models [28] with NN and NNN dimers on the square lattice. [Note that the nature of NNN RVB states in Eq. (1) without the factor $(-1)^{\delta_c}$ remains unknown due to the lack of mapping between them and projected BCS states.]

From the flux pattern $\{\phi_p\}$, we have identified four symmetric NNN RVB states on the square lattice, as is shown in Fig. 3(b). For each of these four states, there is an additional parameter labeling the wave function, namely, the ratio $\gamma \equiv |f_{\mathrm{NNN}}/f_{\mathrm{NN}}|$. We take $\gamma = 1$ in our MC simulations. For $\gamma = 1$, both spin and dimer correlations decay exponentially with distance. The correlation lengths are listed in Table II, where $\xi_{d,\mathrm{NN}}$ and $\xi_{d,\mathrm{NNN}}$ mean the correlation lengths of NN and NNN dimers, respectively. At $\gamma = 1$ (more generally, $\gamma > 0$), we conclude that the four symmetric NNN RVB states are fully gapped Z_2 spin liquids, which is consistent with the recent numerical evidence of fully gapped spin liquids in the J_1-J_2 square Heisenberg antiferromagnet [10,11]. The variational energies of these NNN RVB states in units of J_1 for the J_1-J_2 square Heisenberg model with $J_2 = J_1/2$ are shown in Table II.

Nematic RVB spin liquids.—We have studied fully symmetric short-range RVB spin liquids on various lattices. An interesting question is whether short-range RVB states could be nematic spin liquids which are translationally invariant but break lattice point group symmetry. The answer is yes. On the kagome lattice, we identified that there are only four NN RVB states which are nematic spin liquids, as is shown in Fig. 5(a). On the triangular lattice, there are two nematic NN RVB states, as is shown in Fig. 5(b). Our MC simulations show that the correlation functions of spins and dimers in these states decay exponentially with distance, but the C_{6v} symmetry of both lattices is broken. They are fully gapped nematic spin liquids, in contrast with gapless nematic spin liquids on the triangular lattice studied in Ref. [29].

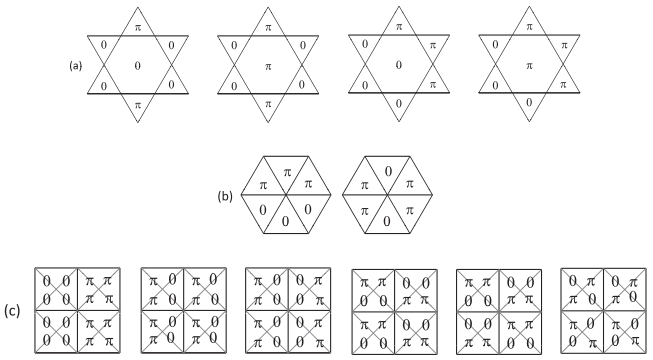

FIG. 5. The flux patterns $\{\phi_p\}$ of (a) the four nematic NN RVB states on the kagome lattice, (b) the two nematic NN RVB states on the triangular lattice, and (c) the six nematic NNN RVB states on the square lattice.

On the square lattice, we found six nematic NNN RVB spin-liquid states, which are shown in Fig. 5(c). These spin-liquid states keep the translational symmetry but break the C_{4v} rotational symmetry of the square lattice. Again, our MC simulations show that they are fully gapped nematic spin liquids.

Concluding discussions.—On the square (or honeycomb) lattice, there are two kinds of symmetric NN RVB spin liquids. The $\{\phi_p = 0\}$ NN RVB state is unfrustrated with power-law decaying dimer correlations [23,24]. For the $\{\phi_p = \pi\}$ NN RVB state, our MC simulations on the square lattice with 40×40 sites implies that its dimer correlation decays in power law, even though we need further studies on systems with larger sizes to determine the power exponent accurately. [Here, the power-law decaying dimer correlations are expected since bipartite RVB states are effectively described by an emergent U(1) gauge theory.]

A recent loop-algorithm MC study shows that the unfrustrated NN RVB states on the cubic and diamond lattices show magnetic long-range order [30]. Properties of NN RVB states on 3D frustrated lattices remain unknown, partly due to the minus sign problem in loop-algorithm MC simulations. We can generalize the mapping between short-range bosonic RVB states and projected BCS states discussed in the present Letter to three dimensions. Consequently, we can solve the minus sign problem for a class of frustrated short-range RVB states, which is a significant step towards understanding the nature of short-range frustrated RVB states in 3D.

We are grateful to Zheng-Yu Weng and Tao Xiang for sharing computing resources and thank Steve Kivelson and Tao Li for helpful discussions. This work is supported in part by the NSFC under Grants No. 10704008 and

No. 11274041 (F. Y.) and by Tsinghua Startup Funds and NSF Grant No. DMR-0904264 (H. Y.).

Note added.—After the completion of the present Letter, we noticed the Letter by J. Wildeboer and A. Seidel studying topics that partly overlap with the present Letter but are from seemingly different approaches [31].

[1] L. Balents, Nature (London) **464**, 199 (2010).

[2] P. W. Anderson, Mater. Res. Bull. **8**, 153 (1973). It is now known that, for antiferromagnetic Heisenberg models on the triangular (or square) lattice with only nearest-neighbor couplings, their ground states have magnetic orders.

[3] P. W. Anderson, Science **235**, 1196 (1987).

[4] S. A. Kivelson, D. S. Rokhsar, and J. P. Sethna, Phys. Rev. B **35**, 8865 (1987).

[5] P. A. Lee, N. Nagaosa, and X.-G. Wen, Rev. Mod. Phys. **78**, 17 (2006).

[6] Z. Y. Meng, T. C. Lang, S. Wessel, F. F. Assaad, and A. Muramatsu, Nature (London) **464**, 847 (2010); D. Zheng, G.-M. Zhang, and C. Wu, Phys. Rev. B **84**, 205121 (2011); S. Sorella, Y. Otsuka, and S. Yunoki, arXiv:1207.1783.

[7] H. C. Jiang, Z. Y. Weng, and D. N. Sheng, Phys. Rev. Lett. **101**, 117203 (2008).

[8] S. Yan, D. A. Huse, and S. R. White, Science **332**, 1173 (2011).

[9] S. Depenbrock, I. P. McCulloch, and U. Schollwoeck, Phys. Rev. Lett. **109**, 067201 (2012).

[10] H.-C. Jiang, H. Yao, and L. Balents, Phys. Rev. B **86**, 024424 (2012).

[11] L. Wang, Z.-C. Gu, F. Verstraete, and X.-G. Wen, arXiv:1112.3331.

[12] R. Moessner and S. L. Sondhi, Phys. Rev. Lett. **86**, 1881 (2001).

[13] R. Moessner, S. L. Sondhi, and E. Fradkin, Phys. Rev. B **65**, 024504 (2001).

[14] The classification here might be closely related to studies based on the projective symmetry group in Refs. [32,33].

[15] N. Read and B. Chakraborty, Phys. Rev. B **40**, 7133 (1989).

[16] S. Yunoki and S. Sorella, Phys. Rev. B **74**, 014408 (2006).

[17] F. Becca, L. Capriotti, A. Parola, and S. Sorella, Springer Ser. Solid-State Sci. **164**, 379 (2011)..

[18] X.-G. Wen, Phys. Rev. B **44**, 2664 (1991).

[19] N. Read and S. Sachdev, Phys. Rev. Lett. **66**, 1773 (1991).

[20] Note that the definition of fluxes above for time reversal invariant RVB states with real f_{ij} is consistent with the more general one on the even-length plaquettes studied in Refs. [33,34].

[21] S. Liang, B. Doucot, and P. W. Anderson, Phys. Rev. Lett. **61**, 365 (1988).

[22] A. W. Sandvik and R. Moessner, Phys. Rev. B **73**, 144504 (2006).

[23] A. F. Albuquerque and F. Alet, Phys. Rev. B **82**, 180408 (2010).

[24] Y. Tang, A. W. Sandvik, and C. L. Henley, Phys. Rev. B **84**, 174427 (2011).

[25] See Supplemental Material at http://link.aps.org/supplemental/10.1103/PhysRevLett.109.147209 for the detailed proof of Eq. (5).

[26] J. Cano and P. Fendley, Phys. Rev. Lett. **105**, 067205 (2010).

[27] H. Yao and S. A. Kivelson, Phys. Rev. Lett. **108**, 247206 (2012).

[28] D. S. Rokhsar and S. A. Kivelson, Phys. Rev. Lett. **61**, 2376 (1988).

[29] T. Grover, N. Trivedi, T. Senthil, and P. A. Lee, Phys. Rev. B **81**, 245121 (2010).

[30] A. F. Albuquerque, F. Alet, and R. Moessner, arXiv:1204.3195.

[31] J. Wildeboer and A. Seidel, preceding Letter, Phys. Rev. Lett. **109**, 147208 (2012).

[32] X.-G. Wen, Phys. Rev. B **65**, 165113 (2002).

[33] F. Wang and A. Vishwanath, Phys. Rev. B **74**, 174423 (2006).

[34] O. Tchernyshyov, R. Moessner, and S. L. Sondhi, Europhys. Lett. **73**, 278 (2006).